# STUDIES ON WETTABILITY OF STAINLESS STEEL 316L POWDER IN LASER MELTING PROCESS

KURIAN ANTONY*, N. ARIVAZHAGAN, K. SENTHILKUMARAN

School of Mechanical and Building Sciences, VIT University, 632014 India
*Corresponding Author: kurianantony@vit.ac.in

**Abstract**

Laser sintering is one of the techniques used in additive manufacturing processes. The main objective of the work is to study the effects of process parameters on wetting phenomenon and interfacial energy during laser melting of stainless steel powder. This paper reports wetting of laser melted powder particles and its use for the determination of surface energy of stainless steel powder under laser beam exposure. Process parameters such as laser power, scan speed and beam diameter are considered for study. This study also identifies the process parameters for better wettability which produces smooth surfaces.

Keywords: Stainless steel, Wettability, Interfacial energy ratio, Macrostructure.

## 1. Introduction

Selective laser melting process enables the fabrication of components with complex shapes directly from metallic powder [1]. Laser melting process has aroused wide concerns and has been widely used in biomedical, aerospace and many other engineering fields, offering a series of advantages compared with traditional processing techniques due to its versatility in producing parts of both metals as well as polymer [2-5]. Moreover Stainless steel 316L (SS316L), is a widely used material in biomedical applications such as orthopaedic pins, plates and hip replacements and is preferred over Ti Alloys for the cost advantage [6]. However, during the Selective Laser Melting (SLM) process, the laser molten track possesses a shrinking tendency to decrease the surface energy under the action of surface tension. Thus, the balling phenomenon is easily observed during SLM process, which is detrimental to the quality of SLM processed part and hinder the further development of SLM technology [7-10].

<div style="border:1px solid">

**Nomenclatures**

| | |
|---|---|
| $d$ | Beam diameter, μm |
| $E$ | Energy density, J/mm$^2$ |
| $P$ | Laser power, W |

***Greek Symbols***

| | |
|---|---|
| $\theta$ | Wetting angle, deg. |
| $\tau$ | Interfacial energy ratio |

</div>

Balling phenomena mainly occurs due to the poor wettability of the powder. Moreover wettability plays a major role in laser melting process which affects the mechanical as well as the corrosion behaviour of the laser melted parts [8]. Poor wettability in the surface produces cracks which will further cause corrosion of the part. Thus the laser melted surface with good wettability is less prone to corrosion and have high wear resistance. To ensure good wetting and successful layer-by-layer consolidation the processing must be conducted in a vacuum or protective atmosphere using high purity inert gases [1].

For better wettability to take place, surface oxide reduction is necessary. De Gennes [11] has given an excellent review of the physical mechanisms governing the wetting. The wetting behavior of a molten liquid on a substrate of its own kind was investigated recently by Schiaffino and Sonin [12-14]. However this particular situation is known as "homologous wetting" and is inherently a non-equilibrium phenomenon involving simultaneous heat transfer, fluid flow and solidification [15]. Moreover poor wettability can leads to balling and crack formation which further leads to lower corrosion resistance and mechanical properties.

This work mainly concentrates on the various process parameters which influence the wettability of the laser melted track.

## 2.   Physical Model

The interfacial energy of the solid-solid and the liquid-solid interfaces is related to wetting angle is as follows [16]:

$$\frac{\gamma_{SL}}{\gamma_{SS}} = \frac{1}{2\cos(\theta/2)} = \tau \tag{1}$$

where $\gamma_{SL}$ and $\gamma_{SS}$ are the energies of the solid-liquid interface and solid-solid grain boundary respectively and $\theta$ is the wetting angle, $\tau$ interfacial energy ratio.

## 3. Experimentation

Experiments were conducted by melting of powder material and forming droplets onto prepared substrates of the similar material to investigate homologous wetting in SLS. Nd: YAG pulsed laser JK 300P (UK) of maximum peak power 5 kW, maximum pulse energy 40 J was used. Nitrogen atmosphere has been maintained in order to prevent oxidation. Schematic representation of the experimental setup is shown in Fig.1.

Stainless steel 316L was chosen as the material for investigation due to its ready availability in both powder and plate form and its virtue of enormous applications. The substrate was prepared by polishing with 120, 240, 400 and 600 abrasive grits, followed by 3µm diamond paste and a final polish with 0.05µm alumina slurry, followed by ultrasonic cleaning in acetone. This preparation technique was necessary to provide as clean and smooth surface as possible since the presence of surface oxides will cause the material to spread poorly [9] and to reduce the influence of surface roughness to the wetting behaviour. For conducting the experiments, taguchi L9 orthogonal array has been followed as shown in Table 1.
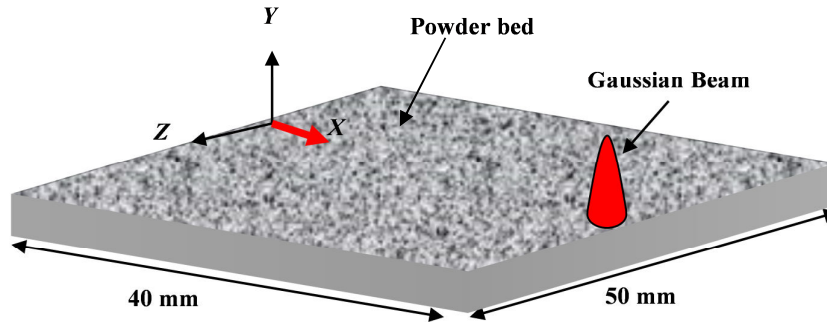


**Fig. 1. Specimen for SS316L Powder Bed Irradiated by Nd-YAG Laser Beam.**

**Table 1. The Selected Process Parameters for
Laser Melting for Making Single Layer Track.**

| Trial No | Laser Power (W) | Laser Speed (m/min) | Beam Dia. (µm) | Energy Density (J/mm$^2$) | Interfacial Energy Ratio ($\tau$) | Wetting Angle ($\theta$) |
|---|---|---|---|---|---|---|
| 1 | 100 | 2.4 | 300 | 8.33 | 0.52543 | 35.8040 |
| 2 | 100 | 8.4 | 400 | 1.785 | 0.61812 | 72.0230 |
| 3 | 100 | 12 | 500 | 1 | 0.52069 | 32.4130 |
| 4 | 150 | 2.4 | 400 | 9.375 | 0.5514 | 24.9360 |
| 5 | 150 | 8.4 | 500 | 2.142 | 0.52377 | 34.6530 |
| 6 | 150 | 12 | 300 | 2.5 | 0.52465 | 35.2680 |
| 7 | 200 | 2.4 | 500 | 10 | 0.51635 | 28.9180 |
| 8 | 200 | 8.4 | 300 | 4.761 | 0.57257 | 58.3250 |
| 9 | 200 | 12 | 400 | 2.5 | 1.37627 | 137.3940 |

Initially, the stainless steel powder was spread over the substrate and maintaining the thickness of 100 µm using scraper blade. Laser moves in *x* direction of the powder bed which produces melted track. Wetting angle is measured with image analyser. In addition energy density of the laser beam is denoted by the following equation [17].

$$E = \frac{P}{vd} \tag{2}$$

where *P* is the laser power used to scan a part; *v* is the scan speed or the velocity by which the laser beam moves over the powder surface, and *d* is the beam diameter.

## 4. Results and Discussion

### 4.1. Experimentation

Sequential images from digital macroscopy of the experiment conducted with stainless steel powder on stainless steel plate are shown in Fig. 2. Figures 2(d), (f), and (g) schematically depicts the formation of continuous scan track, in general at relatively lower scanning speed the powder agglomeration and continuous melting normally occurs. In other words at lower scanning speed powder particles have much time for melting and solidification. Single layer tracks in Figs. 2(a-c), (e), (g) and (h) reveals that the molten powder shows no tendency to spread and wet the underlying substrate. Instead, it formed a nearly spherical droplet having a point like contact with the substrate. Laser melted track which gives large semi-circle droplets as shown in Fig. 2(i) which is having the highest contact angle. This effect justifies that increase in contact angle will leads to poor wettability and thus the quality of the part will get affected.
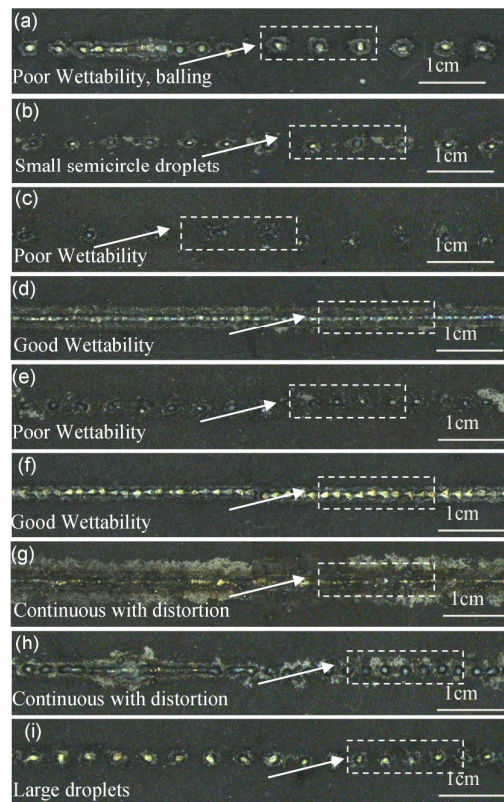


**Fig. 2.The Macrograph of Single Track
Formation of SS 316L Powder on SS 316L Substrate.**

**(a)** *P*= 100 W; *V*= 2.4 m/min; *d*= 300 μm.  **(b)** *P*= 100 W; *V*= 8.4 m/min; *d*= 400 μm.
**(c)** *P*= 100 W; *V*= 12  m/min; *d*= 500 μm.  **(d)** *P*= 150 W; *V*= 2.4 m/min; *d*= 400 μm.
**(e)** *P*= 150 W; *V*= 8.4 m/min; *d*= 500 μm.  **(f)** *P*= 150 W; *V*= 12  m/min; *d*= 300 μm.
**(g)** *P*= 200 W; *V*= 2.4 m/min; *d*= 500 μm.  **(h)** *P*= 200 W; *V*= 8.4 m/min; *d*= 300 μm
**(i)** *P*= 200 W; *V*= 12  m/min; *d*= 400 μm.

## 4.2. Wetting

Table 1 shows the wetting angle and interfacial energy ratio of the nine laser process parameters. Wetting angle is measured with the image analyser; the contact angle for various process parameters is shown in Table 1.

Figure 3 explains the relation between wetting angle and the energy densities of different process parameters. From the graph it is clearly understood that wetting angle increases at the lower energy density level. However it is noted that at lower energy density level the melting of the powder won't happen properly which will leads to distortion further cause's poor wettability. In the case of higher energy density as the laser power increases or the scan speed decreases, the amount of energy absorbed by the powders under the laser beam enhances, inducing a larger degree of melting which causes good wettability. Moreover the Wetting of the grain boundaries by a continuous liquid film occurs for $\tau$ less than $0.5(\theta < 60^0)$ and for values above 0.5, the resistance to cracking increases which will leads to corrosion [18].
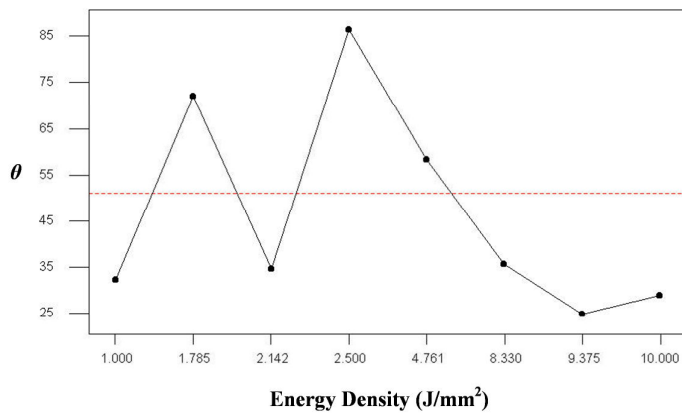


**Fig. 3. Energy Density vs. Wetting Angle.**

Figure 4 shows that interfacial energy ratio has an influence on the energy density of the laser. Figure 5 reveals the effect of different process parameters on wetting; it is evident from the graph that as the laser power increases wettability also increases same as in the case of scanning speed. If the scan speed is higher, due to the pulse separation, the contact on all sides of the droplet becomes solid-liquid in nature. So the wettability is altered primarily because of the speed and pulsing of the laser. However it is noted from Fig. 5 higher the beam size the tendency of wettability is very low, this mainly because of the larger beam which rarely melts the powder particles. From the experimental results the tracks which produce discontinuous as well as large droplets have $\tau$ more than 0.5 and $\theta$ more than $60^{\circ}$.

During wetting process the adhesion between the solid and liquid is greater than the cohesive force of the liquid. For laser melting, wetting implies that the molten powder spreads on the substrate or previously sintered layer, instead of balling up on its surface. The higher the solid–liquid surface energy, the greater is the tendency to minimize the liquid–solid interface by formation of isolated

pockets of liquid instead of continuous films. Borland and Younger [19] showed that the interfacial energy ratio for iron–iron sulphide films was close to 0.5, explaining the deleterious effect of sulphur in steels.
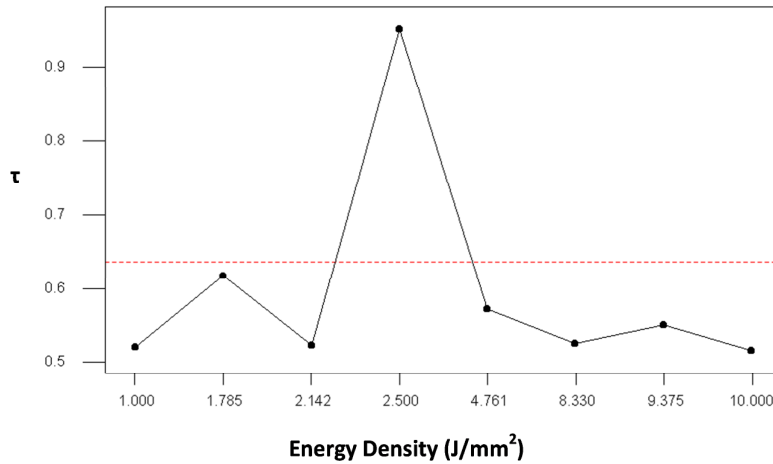


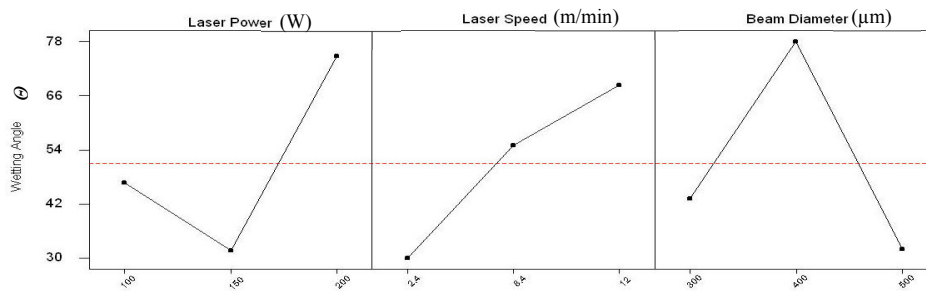**Fig. 4. Energy Density vs. Interfacial Energy Ratio.**



**Fig. 5. Effect of Process Parameters on Wetting.**

## 5. Conclusions

Optimum process conditions for laser melting process to achieve continuous track with good wettability have been investigated with stainless steel powder with different process parameters. Wettability and surface energies of the laser melted stainless steel powder has been found out experimentally. The laser melted track having low contact angle as well as interfacial energy gives good wettability. From all the nine laser parameters used in this study, the set of parameter which gave good wettability as well as smooth and continuous track is of laser power 150 W, scan speed 2.4 m/min, spot size 400 μm. Moreover it is well understood from the ANOVA study that the main process parameters that affects the wettability are laser power and scan speed of laser.

## Acknowledgement

## References

1.  Li, R.; Liu, J.; Shi, Y.; Wang, L.; and Jiang, W. (2012). Balling behavior of stainless steel and nickel powder during selective laser melting process. *International Journal of Advanced Manufacturing Technology*, 59(9-12), 1025-1035.

2.  Yadroitsev, I.; Bertrand, Ph.; and Smurov, I. (2007). Parametric analysis of the selective laser melting process. *Applied Surface Science*, 253(19), 8064-8069.

3.  Li, R.; Shi ,Y.; Liu, J.; Xie, Z.; and Wang, Z (2010). Selective laser melting W-10 wt.% Cu composite powders. *International Journal of Advanced Manufacturing Technology*, 48(5-8), 597-605.

4.  Jhabvala, J.; Boillat, E.; André, C.; Glardon. R. (2011). An innovative method to build support structures with a pulsed laser in the selective laser melting process. *International Journal of Advanced Manufacturing Technology*, 59(1-4), 137-142.

5.  Wang, F. (2011). Mechanical property study on rapid additive layer manufacture Hastelloy®X alloy by selective laser melting technology. *International Journal of Advanced Manufacturing Technology*, 58(5-8), 545-551.

6.  Kurian, A.; Arivazhagan, N.; and Senthilkumaran, K. (2013). Influence of laser melting process parameters on surface roughness behavior for SS316L powder. *Journal of Corrosion Science and Engineering*, 16, Reprint 31

7.  Kruszewski, K.M.; Nistico, L.; Longwell, M.J.; Hynes, M.J.; Maurer, J.A.; Hall-Stoodley, L.; and Gawalt, E.S. (2013). Reducing staphylococcus aureus biofilm formation on stainless steel 316L using functionalized self-assembled monolayers. *Materials Science and Engineering C*, 33(4), 2059-2069.

8.  Gu, D.; and Shen, Y. (2007). Balling phenomena during direct laser sintering of multi-component Cu-based metal powder. *Journal of Alloys and Compounds*, 432(1-2), 163-166.

9.  Kruth, J.P.; Froyen, L.; Van Vaerenbergh, J.; Mercelis, P.; Rombouts, M.; and Lauwers, B. (2004). Selective laser melting of iron-based powder. *Journal of Materials Processing Technology*, 149(1-3), 616-622.

10. Niu, H.J.; and Chang, I.T.H. (1999). Instability of scan tracks of selective laser sintering of high speed steel powder. *Scripta Materilia*, 41(11), 1229-1234.

11. de Gennes, P.G. (1985). Wetting: statics and dynamics. *Reviews of Modern Physics*, 57(3), 827-863.

12. Schiaffino, S.; and Sonin, A.A. (1997). Motion and arrest of a molten contact line on a cold surface: An experimental study. *Physics of Fluids*, 9(8), 2217-2226.

13. Schiaffino, S.; and Sonin, A.A. (1997). On the theory for the arrest of an advancing molten contact line on a cold solid of the same material. *Physics of Fluids*, 9(8), 2227-2233.

14. Schiaffino, S.; and Sonin, A.A. (1997). Molten droplet deposition and solidification at low Weber numbers. *Physics of Fluids*, 9(11), 3172-3187.

15. Das, S. (2001). On some physical aspects of process control in direct selective laser sintering of metals - Part I. *Solid Freeform Fabrication Proceedings*, 85-93.

16. Zener, C. (1948). Grains, phases and interfaces: an interpretation of microstructure. *Transaction of American Institute of Mining, Metallurgical Engineers*, 175**,** 15-51.

17. Lu, L.; Fuh, H.; and Wong, Y.-S. (2001*). Laser-induced materials and processes for rapid prototyping*. Kluwer Academic Publishers, ISBN 0792374002, Norwell, USA.

18. Borland, J.C. (1960). Generalized theory of super-solidus cracking in welds (and castings). *British Welding Journal*, 7, 508-512.

19.  Borland, J.C.; and Younger, R.N. (1960). Some aspects of cracking in welded Cr–Ni austenitic steels. *British Welding Journal*, 7, 22-59.